

Development of an Omnidirectional Power-Assisted Cart

Go Hirano and Kouta Goto

Department of Electric and Electronic Engineering, Kindai University, Fukuoka, Japan

Email: hira@fuk.kindai.ac.jp, 1611170022y@ed.fuk.kindai.ac.jp

Abstract—A power-assisted cart controlled by forces applied from an operator is designed and developed. This cart is capable of determining the intended direction and velocity of the force applied on the handle. An intuitive operation of the cart is incorporated to facilitate the operator's task as the cart moves in any direction. The developed cart is equipped with mehanum wheels so that it can move in any direction. To improve its operability, the movement task is classified into three types. The relationship between these three types and the operation force is determined and the cart's kinematics derived. The derived kinematics are experimented, though an unstable motion selection is observed in some trials. This study reports a methodology that aims to reduce this instability.

Index Terms— power-assisted cart, mehanum wheel, operational force, omnidirectional mobile robot

I. INTRODUCTION

A power-assist cart equipped with an electric motor on a small pushcart enables the transportation of heavy loads without resulting to extra burden carried by the operator. However, the inability of the driving wheels of most of these carts steer makes it relatively difficult to maneuver such systems in a restricted space, since nonholonomic constraints prevent it from undergoing lateral motion. From the viewpoint of operability, non-restricted directional motion is preferred.

A variety of mechanisms have been developed containing holonomic omnidirectional movement mechanisms [1-3]. The omni and mehanum wheels both have a free roller on the outer circumference of the wheel, and each wheel rotates under the influence of a driving force with one degree of freedom. Multi-directional motion is thus possible as a result of the operation of the free rollers by combining the action of three or more wheels. However, these types of wheels are poor at overcoming steps. Using caster-type mechanism, motion in an arbitrary direction can be achieved by driving an offset shaft as well as the wheels of the caster [4-6]. Omnidirectional motion in the ball-type mechanism is achieved by transmitting the driving force in the direction of two degrees of freedom to the spherical wheel [7]. These mechanisms can generate driving force in two degrees of freedom for each wheel, allowing for multi-directional motion if the system has at least two wheels.

To ensure stability, the system should have more than two wheels. Furthermore, each wheel has two motors, which highly complicates the transmission mechanism. The main movements involved in a displacement between two points are along the longitudinal and turning directions, while lateral movement is often used to adjust the position. In such cases, it would appear that the mehanum wheel, which does possess any complex driven mechanisms and control methods, would be suitable. Furthermore, overcoming small steps in the longitudinal direction has proven possible. Fujiwara et al. [8] in a study, realized that longitudinal and turning motions by using a three-axis force sensor to measure the operation force applied by the operator to the handle. However, a rotation movement that changes the altitude of the cart was not implemented. Operability clearly improves with rotation. That is, mobile robots that follow a target person using sensors [9, 10] and robots that operate using a remote controller have been developed. Although these robots are applicable in global transportation, it is difficult to specify its local movements. To operate the cart, the operator has to push it directly.

An intuitively operated power-assisted cart that uses a mehanum wheel, which can undergo multi-directional motion, was developed [11]. The transportation mode was classified into three types including translational, rotational, and turning motions. Following the transportation experimental results, the cart motion sometimes show unstable features. Therefore, this study reports on the conditions required for possible improvement of motion selection. The configuration of the proposed cart as well as its classification into three groups is detailed in section 2, while the cart kinematics for each motion are presented in section 3, and in section 4. In addition, a description of the manner of selection of the above mentioned motions based on the operational force is performed. Moreover, the conditions of the turning motion and control stabilization are described. Section 5 shows the efficacy of the proposed method using the developed cart, while Section 6 concludes this paper.

II. OVERVIEW OF THE OMNIDIRECTIONAL MOBILE CART

A power-assisted cart, with key function to relieve the burden imposed on the operator, was developed. The

shape and size of the developed cart was similar to those of a small conventional pushcart. The cart was equipped with a table for carrying loads, with a capacity of up to 100 kg, and a top speed of 1 m/s. The operator holds the cart's handles and applied a force intended toward the direction of motion. This force is called the "operational force." It is measured using a force sensor attached to the handle of the cart. This enables the cart to recognize the operator's intention and move in the direction corresponding to the magnitude and direction of the applied operational force. Here no peculiar step is assumed in the transporting work. To realize movement in an arbitrary direction and reduce the burden on the operator, the developed cart has mechatronic wheels to move omnidirectionally. The barrel-shaped, free-turning roller also known as the "free roller," surrounds the wheel and inclined at 45° to the driven shaft of the wheel. The mechatronic wheel is capable of executing forward,

backward, lateral, and diagonal movements. Just as in a typical four-wheeled vehicle, the mechatronic wheel is used in sets of four, with the ability to overcome small steps. Each wheel is driven by an individual actuator with movements from the resulting velocity and direction determined by the four wheels.

To reduce the burden imposed on the operator and improve the operability of the cart, the motions of the cart are classified into three categories, which includes translational, rotational, and turning motion. The altitude of the cart remains constant during translational motion (Fig. 1(a)). The rotational motion rotates around the operator (Fig. 1(b)), while the turning motion rotates along a certain turning radius (Fig. 1(c)). Combining these three motions, it is possible to achieve any movement required. The developed cart determines which motion to realize from the operational force applied to the handle of the cart.

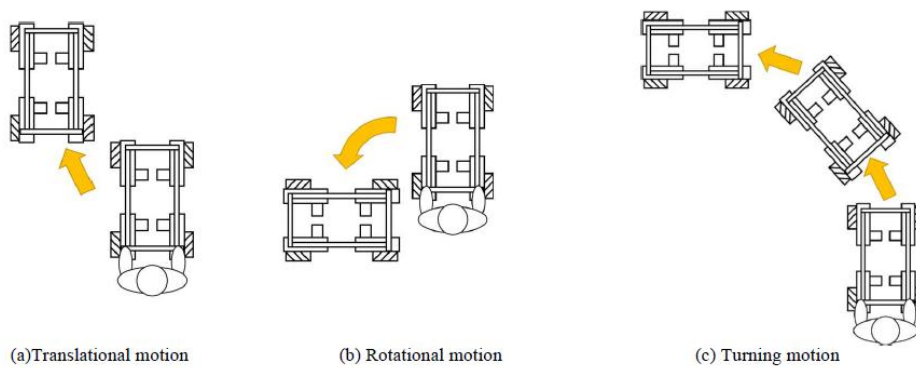


Figure 1. Representation of the three motions.

III. KINEMATICS OF THE CART

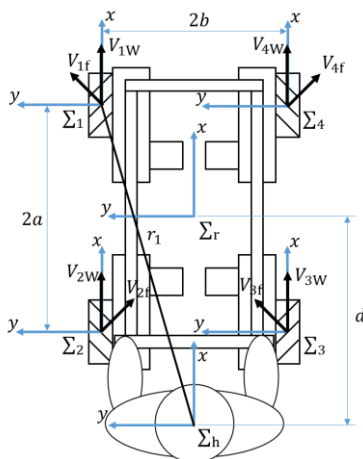


Figure 2. Coordinate system of the cart.

By solving the kinematics of the cart, we obtained values for the wheel velocities, which assisted in realizing the three motions, described above. The operator coordinate system Σ_h is attached to the center of the operator's body (Fig. 2). The desired velocity and angular velocity vectors are applied to Σ_h as $V = (V_x, V_y, \omega)$. This was called the "desired velocity vector." This velocity

vector was provided by the operator. The wheels were numbered from one to four counterclockwise. The wheel coordinate system, which originates from the grounding point of each wheel, is defined as Σ_i ($i = 1-4$). The cart coordinate system, which originates from the center of the cart, is defined as Σ_r . The wheelbase of the cart was defined as $2a$, the tread length as $2b$, the distance from the origin from Σ_r to Σ_h and Σ_h to Σ_i as d and r_i , respectively. The angle of the x-axis of Σ_h and r_i was defined as θ_i . V_{iw} was defined as the velocity vector generated by the rotation of the wheel driven by the actuator, and V_{if} as the tangent velocity vector at the ground point of the free roller. Each wheel moved with a velocity vector $V_i = (V_{ix}, V_{iy})$, which composed of V_{iw} and V_{if} . However, only V_{iw} was controlled by the actuator. The procedure for calculating V_{iw} is shown below.

The free rollers were mounted at an angle of 45°. Given that V_i is determined by V_{iw} and V_{if} , the speed component of each wheel was represented using the following equations:

$$V_{1x} = V_{1w} + \frac{V_{1f}}{\sqrt{2}}, V_{1y} = \frac{V_{1f}}{\sqrt{2}} \quad (1)$$

$$V_{2x} = V_{1w} + \frac{V_{2f}}{\sqrt{2}}, V_{2y} = -\frac{V_{2f}}{\sqrt{2}} \quad (2)$$

$$V_{3x} = V_{1w} + \frac{V_{3f}}{\sqrt{2}}, V_{3y} = \frac{V_{3f}}{\sqrt{2}}, \quad (3)$$

$$V_{4x} = V_{4w} + \frac{V_{4f}}{\sqrt{2}}, V_{4y} = -\frac{V_{4f}}{\sqrt{2}}. \quad (4)$$

Furthermore, each V_i had the following relationship with V :

$$V_{ix} = V_x - r_i \omega \sin \theta_i, V_{iy} = V_y + r_i \omega \cos \theta_i. \quad (5)$$

To summarize (1)–(5), we solve for V_{iw} as follows:

$$\begin{bmatrix} V_{1w} \\ V_{2w} \\ V_{3w} \\ V_{4w} \end{bmatrix} = \begin{bmatrix} 1 & -1 & -r_1(\sin \theta_1 + \cos \theta_1) \\ 1 & 1 & -r_2(\sin \theta_2 - \cos \theta_2) \\ 1 & -1 & -r_3(\sin \theta_3 + \cos \theta_3) \\ 1 & 1 & -r_4(\sin \theta_4 - \cos \theta_4) \end{bmatrix} \begin{bmatrix} V_x \\ V_y \\ \omega \end{bmatrix}. \quad (6)$$

A. Translational Motion

Herein, no change in the cart's altitude was observed, and all the wheel velocity vectors V_i were equal to the desired velocity vector V . Thereafter, $\omega = 0$ was substituted into (6), and then each velocity component of V_{iw} calculated.

B. Rotational Motion

This was realized using the angular velocity ω around the operator. There was no translational motion while the translational velocity components V_x and V_y were set to zero. r_i was calculated from the geometric relationship. Therefore, each velocity component of V_{iw} was computed using (6).

C. Turning Motion

The turning motion is also demonstrated as $V_x = V_y = 0$. The virtual rotation center $P = (P_x, P_y)$ was defined in Σ_h . Rotational motion was then performed with the desired angular velocity ω around P . Herein, $P_x = 0$ was set for the operator to easily perform the turning motion. The calculated distance between P and each coordinate system, and from this and ω , estimated V_{iw} using (6). In the case of $P_y > 0$, V_{iw} is solved using following equation:

$$\begin{bmatrix} V_{1w} \\ V_{2w} \\ V_{3w} \\ V_{4w} \end{bmatrix} = \begin{bmatrix} 1 & -1 & -(a + d - P_y) \\ 1 & 1 & -(a - d - P_y) \\ 1 & -1 & a + 2b - d + P_y \\ 1 & 1 & a + 2b + d + P_y \end{bmatrix} \begin{bmatrix} 0 \\ 0 \\ \omega \end{bmatrix}. \quad (7)$$

When $P_y < 0$, V_{iw} is obtained as follows:

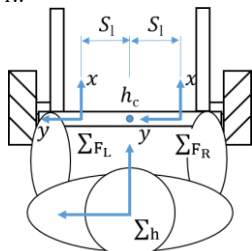


Figure 3. Illustration of operational force coordinate system.

$$\begin{bmatrix} V_{1w} \\ V_{2w} \\ V_{3w} \\ V_{4w} \end{bmatrix} = \begin{bmatrix} 1 & -1 & -(a + 2b + d - P_y) \\ 1 & 1 & -(a + 2b - d - P_y) \\ 1 & -1 & a - d + P_y \\ 1 & 1 & a + d + P_y \end{bmatrix} \begin{bmatrix} 0 \\ 0 \\ \omega \end{bmatrix}. \quad (8)$$

By using these equations, it is possible to determine V_{iw} and realize the required motion. The next section contains information on the selection of the classified three motions using the given operational force.

IV. RELATIONSHIP BETWEEN OPERATIONAL FORCE AND CART MOVEMENT

The operational force applied to the handle determines the desired velocity and direction of the power-assisted cart. The force sensor attached to the handle measured the force applied by the left and right hands of the operator. Two sensor coordinate systems, namely, Σ_{F_L} and Σ_{F_R} (Fig. 3) were set. The force vectors $F_L = (F_{Lx}, F_{Ly})$ and $F_R = (F_{Rx}, F_{Ry})$ were measured in Σ_{F_L} and Σ_{F_R} , respectively. These sensor coordinate systems originate at the distance S_1 from the center position h_c of the handle and are parallel to Σ_h . From the values of the two force sensors, the intended motion of the operator was estimated and the relationship between the operational force and the desired velocity vector was then described.

A. Desired Velocity Vector for Translational Motion

When the signs of F_L and F_R are identical and when the difference between the sizes of F_L and F_R is within F_{limit} , the cart performed translational motion.

$$F_{Lx} > 0, F_{Rx} > 0 \text{ or } F_{Lx} < 0, F_{Rx} < 0, \quad (9)$$

$$|F_{Lx} - F_{Rx}| \leq F_{limit} \quad (10)$$

Under these conditions, the desired velocity components were calculated using the following equation.

$$V_x = \alpha_x \frac{F_{Lx} + F_{Rx}}{2} \quad (11)$$

$$V_y = \alpha_y \frac{F_{Ly} + F_{Ry}}{2} \quad (12)$$

where, α_x and α_y are positive weighting coefficients related to the velocity and operational force.

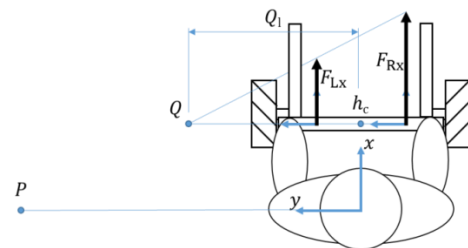


Figure 4. Diagram showing the virtual rotation center.

B. Desired Velocity Vector for Rotational Motion

When the operational force, such as the force rotating around h_c of the handle is given, it is assumed a

rotational motion. This means that the signs of F_{Lx} and F_{Rx} are opposite. Thus, rotational motion occurs under the following two conditions:

$$F_{Lx} > 0, F_{Rx} < 0 \text{ or } F_{Lx} < 0, F_{Rx} > 0, \quad (13)$$

$$|F_{Lx} - F_{Rx}| > F_{limit} \quad (14)$$

In this case, the desired angular velocity was determined by the following equation:

$$\omega = \alpha_r \frac{-F_{Lx} + F_{Rx}}{2} \quad (15)$$

where, α_r is a positive weighting coefficient relating the angular velocity to the operational force. When $F_{Lx} > 0$ and $F_{Rx} < 0$, the cart rotates counterclockwise. Therefore, ω becomes negative. Furthermore, when $F_{Lx} < 0$ and $F_{Rx} > 0$, the cart rotates clockwise and ω becomes positive.

C. Desired Velocity Vector for Turning Motion

In addition to the two cases above, the cart performed a turning motion. This occurred when F_{Lx} and F_{Rx} had the same sign and when there was a difference of more than F_{limit} between these two forces. Firstly, how the position of the virtual rotation center P from the operational force was obtained will be explained. As shown in Fig. 4, a line was drawn through the tip of F_{Lx} and F_{Rx} . The point that intersected this line and the y-axis of Σ_{FL} and Σ_{FR} was set to Q . Then, the length from h_c to Q was set to Q_1 . For which, Q_1 was then calculated from the geometric relationship shown in Fig. 4.

$$Q_1 = \frac{F_{Lx} + F_{Rx}}{F_{Lx} - F_{Rx}} S_1 \quad (16)$$

where, Q_1 is determined to be directly related to the difference between the sizes of F_{Lx} and F_{Rx} . Thereafter, the virtual rotation radius was determined from the length proportional to Q_1 . The position P and the angular velocity ω around P were obtained from the following equation:

$$P_y = k_1 Q_1 \quad (17)$$

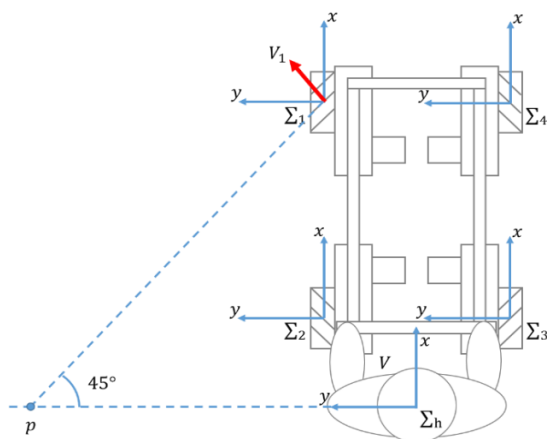


Figure 5. Sketch showing the condition of virtual singular rotation center.

$$\omega = \text{sign}(P_y) \alpha_t \frac{F_{Rx} + F_{Lx}}{2} \quad (18)$$

where, k_1 and α_t are the positive weighting coefficients.

D. Radius Conditions for Turning Motion

Considering that the virtual rotation center P and ω were calculated using (16) - (18), each wheel speed vector V_{iw} was obtained by substituting the kinematic formula described in Section 3.3. When the difference in the size of F_{Lx} and F_{Rx} was large, the turning radius became smaller and P moved closer to the cart during the turning motion. Herein, the case of left turning motion was considered. When the angle between the line connecting P and Σ_1 and the y-axis of Σ_h reached 45° , V_{1w} turned zero (Fig. 5). The wheel velocity V_1 consisted only of V_{1f} of the free roller. Therefore, the driving force generated by the wheel 1 was zero, while the cart moved at the combined speed of the remaining three wheels. The movement became unstable. Assuming P at this condition was a virtual singular rotation center $P_{limit} = (0, P_{y_limit})$, the following relationship was then obtained from the geometrical relationship.

$$P_{y_limit} = a + b + d. \quad (19)$$

For stable motion, P should not be less than P_{y_limit} during the turning motion.

E. Stabilization of the Cart Motion

The translational and rotational motions were selected based on the difference between F_{Lx} and F_{Rx} values as seen in (10) and (14). If this difference continued changing near F_{limit} , a go back and forth movement between these two motions will occur. In the case of the turning motion, the sign of F_{Lx} and F_{Rx} were opposite to that of the translational motion, defining such a problem in valid. Therefore, once the motion was selected, F_{limit} was changed so that another motion was not selected immediately F_{limit} was defined as, a time function that changed with time upon motion selection, and not as a constant. By changing the conditions in this way, a stable transportation was realized by continuing the selected motion. When the translational motion was selected, the new condition F_{limit_t} was once enlarged and converged to its original F_{limit} after a certain time.

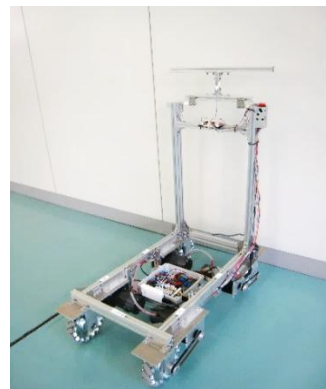


Figure 6. Image of developed power-assisted cart.

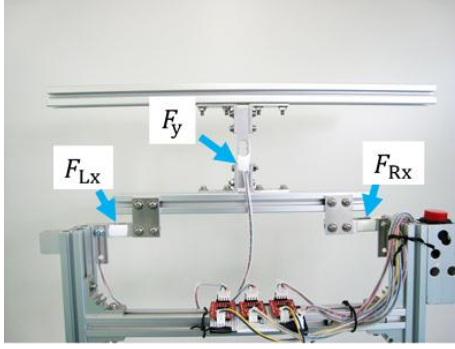


Figure 7. Illustration of the fixed force sensors.

$$F_{\text{limit}_t} = \beta_t F_{\text{limit}} - g(t). \quad (20)$$

where, $F_{\text{limit}_t} \geq F_{\text{limit}}$. When the turning motion is selected, F_{limit_r} was reduced and converged to F_{limit} with progress in time.

$$F_{\text{limit}_r} = \beta_r F_{\text{limit}} + g(t). \quad (21)$$

where, $g(t)$ is an increasing function by elapsed time t after selecting a motion, and $\beta_t > 1$ and $\beta_r < 1$ are constant coefficients.

V. EXPERIMENTAL RESULTS OBTAINED USING THE DEVELOPED CART

To confirm the efficacy of the proposed method, a power-assisted cart (Fig. 6) was developed. The cart length was 0.743 m, and its width was 0.415 m. The handle had a height of 0.95 m. The diameter of the mechatron wheel was 152.4 mm. Four 46 W DC motors were used to drive each mechatron wheel. The other parameters are shown in Table I. A load cell was used to measure the behavior of the operational force for one direction. Therefore, four load cells were required to measure all the operational forces. As described in Section 4, F_{Lx} and F_{Rx} were related to every transport motions, but F_{Ly} and F_{Ry} were only related to the translational motion. Therefore, F_{Ly} and F_{Ry} were measured by a single load cell (Fig. 7), and the measured value of F_y was used for both F_{Ly} and F_{Lx} . An open-loop control and a proportional control method was applied to control the motors. The sampling rate of the force sensor was 10 Hz. The operational force was smoothen by the moving average method using the obtained average sensor value of ten replicates. An increasing function $g(t)$ was set to return to the original F_{limit} value after five seconds. For safety reasons, the theoretical value of P_{y_limit} originally was 1.152 m, but was later set to 1.3 m. Each movement realized by the operational force was confirmed by the following experiments.

TABLE I. PARAMETERS OF THE CART AND COEFFICIENTS

a	0.29 m	α_y	1.3
b	0.16 m	α_r	4.5
d	0.70 m	α_t	3.0
S_l	0.12 m	k_l	10.0
F_{limit}	3.00 N	β_t	1.4
α_x	7.00	β_r	0.7

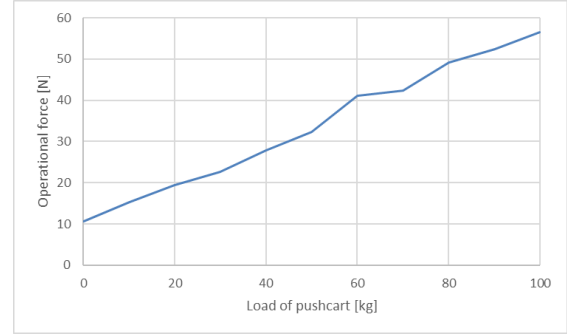


Figure 8. A plot of the relationship between operational force and load.

A. Determination of Upper Limit of Operational Force

Firstly, the amount of operational force required to operate the power-assisted cart was determined. This was performed using a conventional pushcart without power assistance. The size was the same as that of the proposed cart. The force required to move a pushcart was measured by changing the load on the table. Fig 8 shows the average value of the operational force measured multiple times under different load conditions. A pushcart was translated in the x-axis direction of \sum_h at a constant velocity. It was observed that the operational force increased in proportion to the load. Operating the cart with a constant operational force under any load was considered a better option. It was thus made possible to operate the cart with operational force of 12 N or less. Herein, the cart reached its maximum speed at 1 m/s when the operational force was 12 N regardless of the load.

B. Transportation Experiment I

An experiment wherein the cart was translated forward was also conducted. The measured operational forces for this motion are shown in Fig. 9, and the profiles of the corresponding wheel velocity V_{iw} in Fig. 10. Here, V_{iw} values were not experimentally determined, but calculated by kinematics. During translational motion, the difference between F_{Lx} and F_{Rx} was less than F_{limit} . Furthermore, F_y superseded the dead zone momentarily, but was reduced in the process of smoothing the operational force. So, no lateral movement was recorded. It was confirmed that the cart had a maximum speed input when $F_{Lx} + F_{Rx}$ exceeded 12 N in Fig. 10.

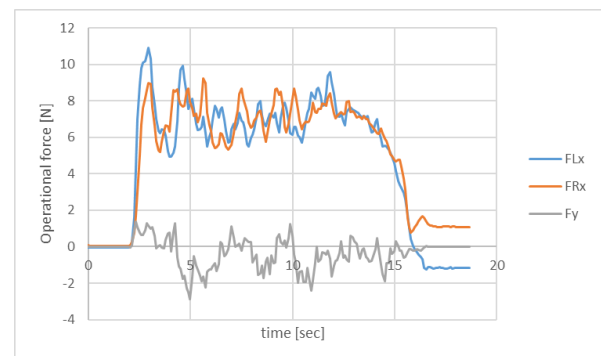


Figure 9. Operational force profiles of Experiment I.

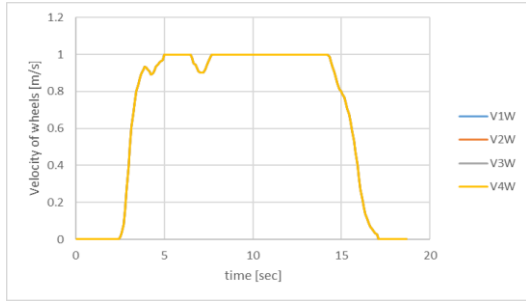


Figure 10. Wheel velocity profiles for Experiment I.

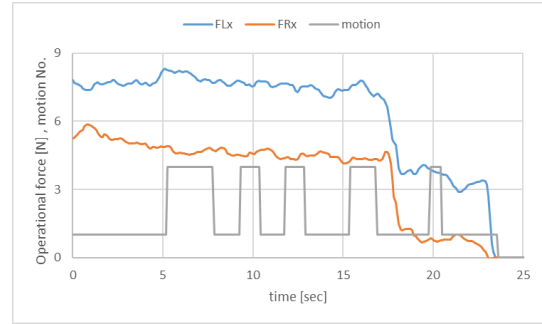


Figure 13. Motion selection without stabilization.

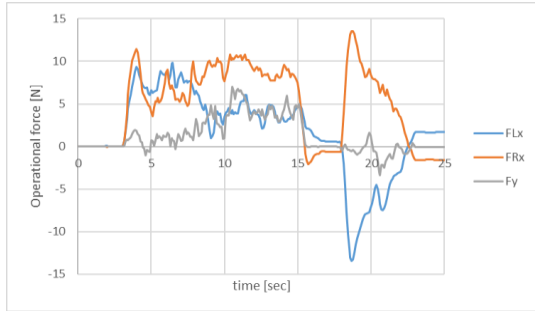


Figure 11. Operational force profiles of Experiment II.

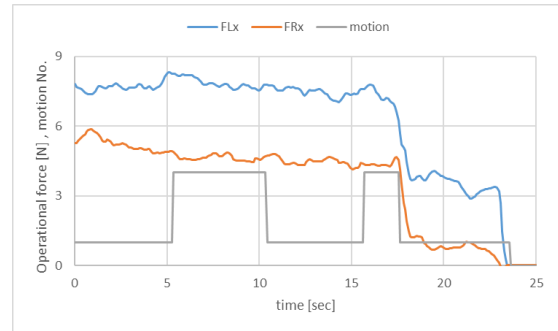


Figure 14. Motion selection with stabilization.

C. Transportation Experiment II

The operational force shown in Fig. 11 was then applied. The velocity profiles are shown in Fig. 12. From 4 to 8 sec, translational motion was performed. Then the cart was turned counterclockwise between 8 and 16 sec. Subsequently, motion was implemented when the difference between F_{Lx} and F_{Rx} was greater than F_{limit} . The cart was observed to occur in rotational motion between the 18th and 23rd sec. The operational force during transportation fluctuated considerably. However, the cart's speed was mildly affected because of the smoothing of the operational force. From this experimental results, it was confirmed that three motions were selected by applying the appropriate operation force.

In addition, when the difference between F_{Lx} and F_{Rx} changed near F_{limit} during translation, the cart chose the turning motion for a moment (Fig. 13). The motion number in this figure means stop at zero, translational motion at one, and turning motion at four. Fig. 14 shows the outcome of applying the operational force with the method of section 4.5. The movement of the cart did not change frequently using proposed method.

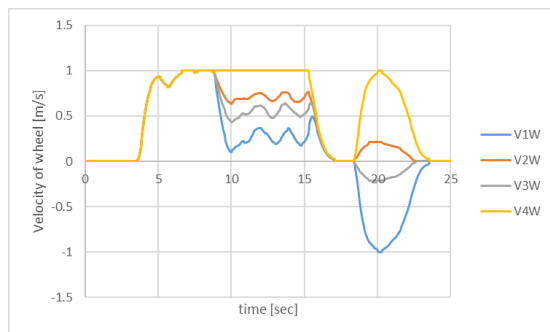


Figure 12. Wheel velocity profiles for Experiment II.

VI. CONCLUSION

In this study, a power-assisted cart with possible control movement by applied operating force was developed. The motion of the cart was classified into three categories including translation, rotation, and turning motion. The relationship between the three types of motions and the corresponding operational force was described, as well as the kinematics of the cart to achieve each classified motion was calculated. An effort was performed to stabilize the motion by adding the condition for the motion selection. Finally, the efficacy of the proposed method was confirmed.

CONFLICT OF INTEREST

The authors declare no conflict of interest

AUTHOR CONTRIBUTIONS

Dr. Hirano supervised the research, derived the formula and wrote a paper; Mr. Goto experimented and analyzed; all authors had approved the final version.

REFERENCES

- [1] A. Yamashita, H. Asama, T. Arai, J. Ota, and T. Kaneko, "A survey on trends of mobile robot mechanisms," *Journal of the Robotics Society of Japan*, vol.21-2, pp. 282-292, 2003(in Japanese).
- [2] F. G. Pin and S. M. Killough, "A new family of omnidirectional and holonomic wheeled platforms for mobile robots," *IEEE Trans. on Robotics and Automation*, vol.10-4, pp.480-489, 1994.
- [3] P. F. Muir and C. P. Neuman, "Kinematic modeling for feedback control of an omnidirectional wheeled mobile robots," in *Proc. IEEE Int. Conf. on Robotics and Automation*, pp. 1772-1778, 1987.
- [4] Y. Ueno, K. Terashima, H. Kitagawa and K. Kakiyama, "Control system of omni-directional mobile robot with caster drive

- mechanism to develop reduction of motor output,” in *Proc. 15th Int. Conf. on Climbing and Walking Robots and Support Technologies for Mobile Machines*, pp.11-18, 2012.
- [5] G. T. Bae, S. W. Kim, D. Choi, C. Cho, W. S. Lee, and S. C. Kang, “Omni-directional Power-assist-modular(PAM) mobile robot for total nursing service system,” in *Proc. 14th Int. Conf. on Ubiquitous Robots and Ambient Intelligence*, pp.832-834, 2017.
- [6] Y. Ueno, Y. Oba, and Y. Matsuo, “Collision avoidance support for a power-assisted omni-directional mobile robot to present obstacle information by adjusting model viscosity coefficients,” *Stics43rd Annual Conference of the IEEE Industrial Electronics Society*, pp. 8491-8496, 2017.
- [7] M. West, H. Asada, “Design of ball wheel mechanisms for omnidirectional vehicles with full mobility and invariant kinematics,” *Journal of Mechanical Design*, vol. 119, pp. 153-161, 1997.
- [8] S. Fujiwara, H. Kitano, H. Yamashita, H. Maeda, and H. Fukunaga, “Omni-directional cart with power assist system,” *Journal of Robotics and Mechatronics*, vol. 14-4, pp. 333-341, 2002.
- [9] M. Gupta, S. Kumar, L. Behera, and V. K. Subramanian, “A novel vision-based tracking algorithm for a human-following mobile robot,” *IEEE Transactions on Systems Man and Cybernetics system*, vol.47-7, pp.1415-1427, 2017.
- [10] T. Ogino, M. Tomono, T. Akimoto, and A. Natsumoto, “Human following by an omnidirectional mobile robot using maps built from laser range-finder measurement,” *Journal of Robotics and Mechatronics*, vol. 22-1, pp. 28-35, 2010.

- [11] G. Hirano, “Control method for a power-assisted cart based on operational force,” in *Proc. of IASTED Int. Conf. on Intelligent systems and control*, 858-013, 2018

Copyright © 2020 by the authors. This is an open access article distributed under the Creative Commons Attribution License ([CC BY-NC-ND 4.0](https://creativecommons.org/licenses/by-nc-nd/4.0/)), which permits use, distribution and reproduction in any medium, provided that the article is properly cited, the use is non-commercial and no modifications or adaptations are made.



Go Hirano was born in Fukuoka, Japan, in 1969. He received BS and PhD in Engineering from Kyushu University in Fukuoka, Japan in 1993 and 2006, respectively. He worked as research associate at Kyusyu University in 1993. Then, he joined Kindai University in Fukuoka, as a lecturer from 2006. He is currently an associate Professor of the Department of Electric and Electronic Engineering,

Kindai University. His research interests in mobile robot, rescue robot and human-robot cooperation. Dr. Hirano is currently a member of The Japan Society of Mechanical Engineers (JSME) and The Robotics Society of Japan (RSJ).



Kouta Goto is undergraduate student, studies in Kindai University since 2016. His research topics are focused on development of omnidirectional mobile robot.